Neutron crystallography – Then and now*

R. Chidambaram and S. K. Sikka†

Neutron crystallography began to be employed at the Bhabha Atomic Research Centre (BARC), Trombay, Mumbai in the early sixties. At that time, the technique, at BARC as well as elsewhere, was in a nascent state, with emphasis on building of instruments and development of crystallography software. Over the years, the Trombay group kept pace with the advancements in other parts of world and employed neutron diffraction to get answers to a variety of important problems. Here we review the advances of the method over the years and its applications. In particular, we discuss the phase problem in neutron crystallography and its contributions for hydrogen bonding, biological macromolecular structures and high pressure science.

FOR the last fifty years, neutron crystallography has been used successfully mainly to study (i) hydrogen atoms in the presence of heavy atoms, and (ii) microscopic magnetic structures and occasionally to distinguish between neighbouring elements in the periodic table. In this article, we focus on the former. The complementary technique of X-ray diffraction, more widely used in structural analysis, has limitations for the above applications. These limitations arise due to difference in the nature of interaction of the two probes with atoms. X-rays are scattered by electrons and thus, higher the atomic number, stronger the scattering. Neutrons on the other hand, are scattered essentially by nuclei and thus the neutron scattering amplitudes have slower variation across the periodic table.

Now it has been shown that the hydrogen atoms can also be located by state-of-the-art X-ray crystallography at synchrotron sources, albeit not so precisely. Since neutrons and X-rays are scattered by different constituents of the atom, they locate centroids of the respective scattering densities. It is well established that there can be considerable differences in neutron scattering density and electron density centroids. For hydrogen, it is typically ~ 0.1 Å. Thus the X–H covalent bond lengths are often underestimated when a structure is determined by X-ray diffraction. In proteins and large molecules, a resolution of about ~ 1 Å is required to see hydrogen atoms individually and considerable effort may be required to achieve this[1]. On the other hand, it has been established for biomacromolecules that neutron data up to 2 Å resolution are sufficient. Moreover, there is no risk of radiation damage in the latter case, which also has been shown to have serious effect on hydrogen atoms, especially on dynamically disordered ones, in high-resolution X-ray studies of proteins.

Ramaseshan is an icon for Indian crystallographers. When one of us (R.C.) joined the Indian Institute of Science, Bangalore in 1956, the ambience there for physics research was perhaps the best in the country at that time, and it was in no small measure due to the presence of eminent people like Ramaseshan in the Department of Physics. His encouraging attitude, his enlightened outlook, the enthusiasm of his group in solving crystal structures (those were early days in X-ray crystallography) and looking at the phase problem using anomalous scattering and in building instrumentation for research played a role in one of the author's (R.C.) changing career direction. The other author (S.K.S.) was inspired by Ramaseshan's paper in *Current Science* in 1966 on neutron anomalous scattering[2], in planning and doing experiments to test the feasibility of using neutron resonance scattering for solving crystal structures.

Phase problem in neutron crystallography

The nuclear scattering length for neutrons can be written as

$$b = b_0 + b' + ib''. \quad (1)$$

The term b_0 represents the hard sphere scattering contribution and is independent of neutron energy. b' and b'' are the energy-dependent potential scattering contributions. b'' is only large when the incident neutron energy is close to a resonance in the target nucleus. It is the term b' that makes the neutron scattering amplitude an irregular but featureful function of the atomic number.

Equation (1) is similar to

$$f = f_0 + \Delta f' + i\Delta f'', \quad (2)$$

the X-ray scattering factor of an atom. $\Delta f'$ and $\Delta f''$ are significant only when the wavelength of the radiation is close to the absorption edge of the atom.

*Dedicated to Prof. S. Ramaseshan on his 80th birthday.

R. Chidambaram and S. K. Sikka are in the Office of the Principal Scientific Adviser to the Government of India, Vigyan Bhawan Annexe, Maulana Azad Road, New Delhi 110 011, India; R.C. is also in Bhabha Atomic Research Centre, Trombay, Mumbai 400 085, India.
†For correspondence. (e-mail: sksikka@nic.in)

The values of b and f for some elements are compared in Table 1. A number of similarities and differences between neutron and X-ray techniques may be recognized in the context of the phase problem.

(i) There are no 'heavy atoms' in neutron scattering. Thus, the application of methods based on Patterson synthesis becomes more difficult. Further, as the value of b for hydrogen is comparable to other elements, there are more atoms to be located at the phase determination stage in a neutron structure analysis. Therefore, the neutron Patterson map will be more crowded. However, in a few cases, superposition methods have helped[3,4].

(ii) The X-ray scattering factors are all positive while for neutrons they are of both signs. Till the late sixties, the negativity of b appeared to rule out the possibility of using direct methods in neutron diffraction, as negative b hydrogen nuclei are present in almost every interesting crystal. This led Karle[5] to propose the squared structure approach to circumvent the problem. It was Sikka[6], in 1969, who finally challenged the view that positivity was the key factor for applicability of direct methods. He showed that the average neutron scattering from hydrogen atoms is rarely more than 30% in a crystal and for this situation, the basic direct-method phase relations are valid. This was soon verified by a number of crystal structure solutions directly from neutron data (e.g. L$_s$-threonine[7], L-proline monohydrate[8] and molepodin, $C_{21}H_{24}O_9$ (ref. 9)) More recently, Hauptman and Langs[10] applied their shake-and-bake algorithm in a straightforward fashion to solve the structure of 199-atom cyclosporin ($C_{62}H_{111}N_{11}O_{12}\cdot H_2O$). In comparison to the deuterated cyclosporin, where all atoms have positive b values, fewer cycles of refinement of phases were required. The authors suggest that the positivity of scattering density might actually be a hindrance for the application of direct methods.

(iii) The neutron scattering amplitudes vary from isotope to isotope of the same element. This allows the use of isotopic replacement, like the conventional isomorphous replacement method, provided one is able to locate the positions of the replaceable atoms. An early application of the isotopic replacement method was on indo-phenyl-2-endo norbornarial (60 atoms in the asymmetric unit). For this compound, Johnson[11] collected the data on two crystals – one containing hydrogen atoms and the other in which four of the hydrogen atoms had been replaced by deuterium atoms. He then employed $(\Delta|F|)^2$ synthesis of Rossmann[12] to locate the replaceable atoms and difference Patterson to find additional atoms. The opposite sign of b values for hydrogen and deuterium has also allowed contrast variation studies to enhance the contribution of specific parts of a molecular substance using different amounts of H and D substitutions.

(iv) The neutron scattering amplitudes for some nuclei like ^{113}Cd, ^{149}Sm, ^{155,157}Gd, ^{135}Xe, etc. which have high resonant absorption for thermal neutrons, are complex and hence the anomalous dispersion method of X-rays should become applicable in neutron diffraction also[13]. However, there are quantitative differences in the values of real and imaginary dispersion terms for the two radiations[2,14] as shown in Table 2 for ^{113}Cd and in Figure 1 for Sm^{149}.

The neutron values of these ratios are an order of magnitude higher than those of the X-rays and vary significantly with wavelength. This suggested that the larger anomalous dispersion effect for neutrons could, therefore, be used to tackle more complex structures than was possible by X-ray anomalous dispersion method. In spite of the higher power of this technique in neutron structure

Table 1. Neutron and X-ray scattering amplitudes for some elements

Element	b (10^{-12} cm)	$f(q = 0)$
H	– 0.374	1
b‡	1.04	
b_-	– 4.07	
D	0.667	1
C	0.665	6
N	0.936	7
O	0.580	8
Cl	0.958	17
^{113}Cd	0.725 + 4.507i (at λ = 0.678 Å)	48
^{149}Sm	0.795 + 6.051i (at λ = 0.915 Å)	62
Dy	1.69	66
U	0.842	92

b‡ for I + ½ and b_- for I – ½ compound nucleus states.

Table 2.

	b'/b_0	b''/b_0
X-rays	~ 0.3	~ 0.3
Neutrons (^{113}Cd)	7.4 at λ = 0.55 Å – 7.4 at λ = 0.8 Å	12.4 at λ = 0.68 Å

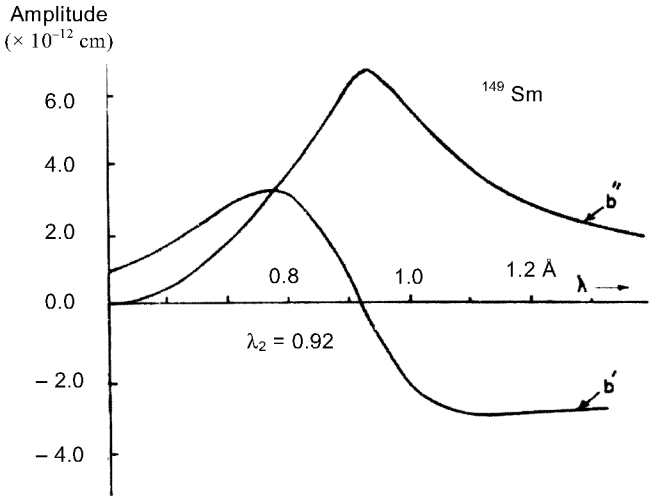

Figure 1. b' and b'' for ^{149}Sm versus wavelength, λ (Å).

analysis for large crystals like proteins, the method has not lived up to its early promise. So far, the method has been used on six small structures and one protein, myoglobin (Table 3).

Most of the techniques of X-ray anomalous scattering have been tested in the above investigations. These include double-phased Fourier synthesis, sine Patterson technique, use of multiwavelength methods, now called MAD, Rossman method[12] for location of anomalous scatterer and integration of direct and anomalous dispersion technique to resolve the phase ambiguity[15]. However, the method has not been used since the end of the seventies. It is beset with the problem of large time required for data collection due to higher absorption of neutrons in crystals containing anomalous scatterers.

It is clear from the above that not many structures have been solved directly from neutron data since the 1980s. This may be attributed to the fact that structure analysis by X-rays at synchrotron sources has become fast. Thus, the positions of non-hydrogen atoms in a crystal are readily available or may be determined quickly before the start of a neutron diffraction study of that substance. The phases calculated from this heavy-atom skeleton of the structure then serve as the starting set. The methods discussed above will become useful only when higher neutron fluxes on samples are possible in future.

Neutron studies on hydrogen bonded systems at Trombay

Our interest in the hydrogen-bonded systems has led to the development of the neutron diffraction technique at the Bhabha Atomic Research Centre (BARC), Trombay since 1960s (ref. 16). Studies started at the CIRUS reactor with a flux of 5×10^{13} neutrons/cm^2/s. The earlier powder and single-crystal diffractometers, which were manual/semi-automatic, were converted into well-engineered, high-precision, computer-controlled diffractometers[17]. In 1987, the higher flux (1.8×10^{14} neutrons/cm^2/s) *Dhruva* reactor became available. Figure 2 shows some of the neutron scattering instruments around this reactor.

The initial work was on the structure and hydrogen-bonding properties of water molecules in the crystals. The 'one-sixth hydrogen' model in the structure of ice-Ih[18], based on the idea that energy penalty for the bending of a hydrogen bond is less than that for the distortion of the HOH angle, was not only more consistent with the neutron data compared to the 'half-hydrogen' model[19], but also in better agreement with the spectroscopic and proton magnetic resonance (PMR) results. The concept of bent hydrogen bonds in water molecules was pursued further using PMR and neutron data from studies on crystal hydrates[20]. Neutron diffraction studies were carried out at Trombay on a number of crystal hydrates, and using the results from these and other studies carried out elsewhere, a classification of the lone-pair coordination of the water molecule was proposed[16]. The Lippincott–Schroeder semi-empirical potential function was modified to account for the bending of hydrogen bonds, and potential functions for bent O–H···O, and N–H···O hydrogen bonds were proposed[21,22]. The next phase of work was on the high-precision neutron studies of amino acids and small peptides. A number of such studies[23,24] and references therein have been carried out at BARC, India; BNL, USA and elsewhere. Many of these structures have been analysed to obtain systematics of molecular structure, conformation and hydrogen bonding of amino acids and small peptides. These have served as inputs to molecular dynamics and energy minimization studies of macromolecules.

A typical hydrogen bond, X–H···Y is characterized by the four essential parameters: the X–H, H···Y, X···Y distances, and the bending angle HXY (inset, Figure 3). In addition, one or two angle parameters may be needed to specify the H-bond orientation with respect to the lone-pair configuration on the acceptor atom. In earlier studies[23], results have been presented on the distributions of many of these parameters, inter-parameter connections, semi-empirical potential functions, standard values for bond distances and angles involving H-atoms, and others. In the subsequent analysis by several authors, many of these parameters have been updated using an enhanced dataset. However, in most cases, the differences are not very significant. For example, from the available neutron diffraction data up to 1968, Chidambaram and Sikka[21]

Table 3.

Structure	Reference
$Cd(NO_3)_2.4D_2O$	55
$Sm(BrO_3)_3.9H_2O$	56
NaSm (EDTA).$8H_2O$	57
Cd(tartrate).$5H_2O$	58
Cd-Histidine.$2H_2O$	59
agua (L-glutamato)Cd(II).H_2O	60
^{113}Cd myoglobin	61

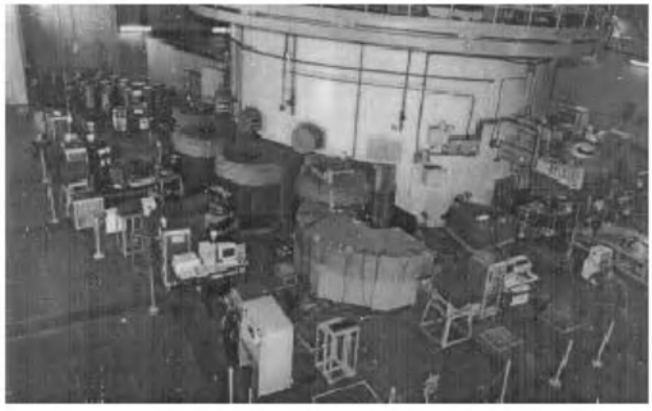

Figure 2. Some neutron scattering instruments around the *Dhruva* reactor at BARC.

derived an inverse correlation between O···O distance and HXY angle (Figure 3). According to this, short hydrogen bonds were more close to linearity. Subsequently, many authors have confirmed this. In particular, see Olovsson and Jonsson[25], Savage and Finney[26] and Steiner and Saenger[27]. They have replaced O···O distance by H···O distance in their plots.

From the hydrogen bond populations associated with the structures of amino acids and peptides, Chidambaram and Ramanadham[28] have carried out an analysis to determine the hydrogen bond formation capabilities of the oxygen atom acceptors in different chemical groups. Bond-valence concept of Brown and co-workers[29] has been employed. Simply, the procedure consists of the computation of the covalent bond strength, in valence units for an oxygen atom, and the amount by which it falls short from two is taken as a measure of its H-bond accepting capability. Results of their analysis are summarized in Table 4, which agree with observed number of hydrogen bonds. Some examples illustrate the usefulness of this approach. In Table 4, the average covalent strength of the –OH oxygen in –COOH groups is 1.95(4) valence units, which hardly leaves any residual valence on this atom for it to accept a hydrogen bond. It is also evident from the table that oxygen atoms O_1 and O_2 of the –COO– group are better hydrogen acceptors than O_1 of the –COOH group. They have applied the above hydrogen bonding criteria to find out the protonation status of GLU35 and Asp32 in lysozyme structure as determined by X-rays[30]. The conclusion that only GLU 35 was protonated has been confirmed by a subsequent neutron study by Mason *et al.*[31] at pH 5.0 (see later in the article).

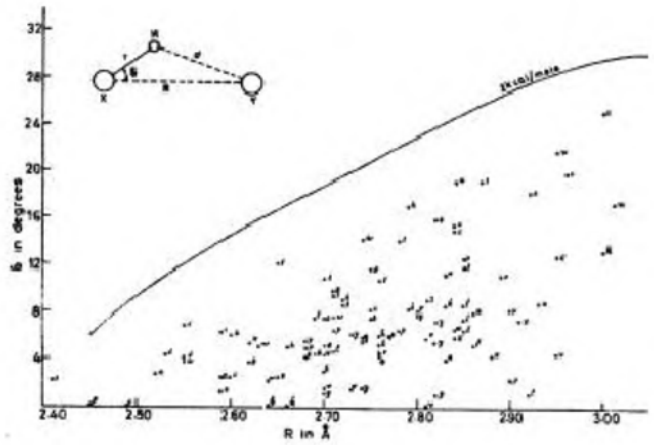

Figure 3. The relationship between δ (angle of bend) and R(O···O) for O_2–H···O hydrogen bonds. Solid line represents an equi-energy contour evaluated from the bent-hydrogen bond potential function in ref. 21.

Biological neutron crystallography

Neutron diffraction study of biomolecules is important for location of specific hydrogen atoms, such as those involved in reaction mechanisms or in their hydration structure. After initial enthusiasm in the 1970s (ref. 32), the use of neutron crystallography for direct determination of hydrogen-atom positions in macromolecules waned considerably. The main reason was the intensity available even at the strongest neutron source such as ILL, which is orders of magnitude weaker than even a laboratory X-ray source. Even with large crystals, one needed data collection times lasting several months. The situation is perhaps changing now with the advent of pulsed neutron sources, use of Laue technique for data collection, advances in neutron detectors and use of software to decompose overlapping spots.

Table 4. Average bond strengths of oxygen atoms in various hydrogen bonding groups. $\langle s(\mathrm{COV})\rangle$ $\langle s(\mathrm{HB})\rangle$ are respectively, average covalent and hydrogen bond strengths, and $s(\mathrm{HB})_{max}$ is the largest H-bond strength of an oxygen atom in each sample (v.u., valence unit)

H-bonding group	$\langle s(\mathrm{COV})\rangle$ (v.u.)	$\langle s(\mathrm{HB})\rangle$ (v.u.)	No. of H-bonds/ no. of oxygen atoms	$s(\mathrm{HB})_{max}$ (v.u.)
	1.70(6)	0.13(6)	14/16	0.27
	1.95(4)	0.00	0/16	0.00
	1.50(4)	0.30(8)	35/21	0.53
	1.48(4)	0.38(10)	42/21	0.54
	1.55(3)	0.25(8)	11/7	0.34
	1.78(2)	0.18(10)	2/2	0.26
	1.71(6)	0.15(5)	6/5	0.18
H_2O	1.65(6)	0.24(8)	14/11	0.35
SO_3^- and SO_4^{2-}	1.63(10)	0.32(13)	13/7	0.53

Hydrogens comprise about half of the atoms in a biomolecule. Because a hydrogen nucleus has a large incoherent neutron scattering cross-section, a high background results in the diffraction experiment. Further, as mentioned earlier, the coherent scattering length of hydrogen is negative and about half in magnitude compared to that of positively scattering C, N and O atoms. Because of this, at medium resolutions available at present, there is a partial cancellation of the hydrogen density from its covalently-bonded C, N and O atoms. The problem is further compounded by series termination errors. This may lead to ambiguities in interpretation. Fong *et al.*[33] and Ostermann *et al.*[34] have demonstrated that the above problems can be overcome by the use of deuteration.

At ILL, LAD1 experimental station[35] uses cold neutrons with a wavelength band around 3.5 Å and $\Delta\lambda/\lambda \sim 20\%$ in quasi-Laue geometry. An imaging plate detector with a neutron sensitive screen of Gd_2O_3 is employed. A number of exposures are taken by rotating the crystal to different positions in order to cover a wide region of reciprocal space. The resolution limit is around 1.5 Å, which is found to be adequate, as most of the crystals studied so far have diffracted up to ~ 2 Å only. Another reactor-based single-crystal instrument has been set-up at JAERI in Japan[36]. It utilizes a bent crystal Si monochromator to obtain high neutron intensity on the sample and imaging plate for data collection. Diffraction data have been collected from rubredoxin and myoglobin in about a month.

At the pulsed neutron sources, the Laue diffraction technique uses a fixed single crystal exposed to a white neutron beam. A time-of-flight method is employed for wavelength-sorting. Pulsed neutron spallation source-based single-crystal instruments are already in operation at the Intense Pulsed Neutron Source (IPNS) in Argonne; Los Alamos Pulsed Neutron Source (LANSCE), the Neutron Scattering Facility KENS at KEK (Japan) and ISIS in Rutherford Appleton Laboratory. Two other sources are under construction: the Spallation Neutron Source (SNS, 1–2 MW) in Oak Ridge and the Japan Spallation Neutron Source (JSNS, 1 MW). A 5 MW European Spallation Source (ESS) is also proposed. This would result in a peak flux about 100 times that of the average flux at ILL. Tanaka *et al.*[37] estimate that it will be possible to determine about 20 structures of biocrystals per year on an average at 1 MW operation. This may be compared with about one structure per day at a 3rd generation X-ray synchrotron source. This means that the neutron technique has to be limited to find specific answers to important problems.

It is clear from the above that the neutron diffraction technique for biocrystals is at present undergoing rapid evolution. Only a handful of structures have been solved so far (Table 5). However, it has already produced some answers. For example, the question of which of the two amino acids in trypsin, Asp102 or His57, is protonated was answered by the neutron study by Kossiakoff and Spencer[38]. Similarly, the neutron structure of hen white lysozyme at pH 7.0 determined to 2.0 Å, showed that neither of the catalytic residues Glu35 or Asp52 was protonated, while earlier neutron study at pH 5.0 had shown that Glu35 was protonated[39].

In India, there is yet no pulsed neutron spallation source. However, there is a possibility for building such a source under the programme, Accelerator Driven Sub-Critical System (ADS) of the Department of Atomic Energy, New Delhi. Till it comes about, Indian scientists should be encouraged to use sources abroad.

Neutron crystallography under pressure

Here powder diffraction is the preferred technique. The requirement of large powder samples in a neutron experiment has limited the applications and pressure range at reactor sources. However, the availability of pulsed

Table 5. Protein structures solved/refined using single-crystal neutron diffraction data, the coordinates for which are available from the current release of Protein Data Bank (PDB) dated 02-09-03

Submission date/ PDB code	Protein	Amino acid residue	Number of atoms in the asymmetric unit	D_{min} (Å)	Wavelength/ method
27-FEB-02, 1IU6	Rubredoxin (mutant)	53	847	1.6	Monochromatic
21-FEB-02, 1L2K	Sperm whale met-myoglobin	153	2717	1.5	Monochromatic
20-AUG-01, 1GKT	Endothiapepsin	329	5171	2.1	Quasi-Laue
14-JAN-01, 1IO5	Hew lysozyme	129	2714	2.0	Quasi-Laue
26-OCT-99, 1C57	Concanavalin A	237	4011	2.4	Quasi-Laue
04-AUG-99, 1CQ2	Sperm whale myoglobin	153	2754	2.0	Monochromatic
23-MAR-99, 1LZN	Hew lysozyme	129	2457	1.7	Quasi-Laue
11-OCT-89, 2MB5	Myoglobin (carbonmonoxymyoglobin)	153	2867	1.8	Mono (!)
14-OCT-88, 3INS	Zn-insulin (dimer)	51	1965	1.5/2.2	X-ray/neutron refinement
16-SEP-87, 1NTP	Beta trypsin	223	3242	1.8	Mono (!)
25-FEB-86, 6RSA	Ribonuclease A complex	124	2246	2.0	X-ray/neutron refinement
29-APR-85, 5RSA	Ribonuclease A	124	2268	2.0	X-ray/neutron refinement

neutron sources has given a flip to the neutron studies under pressure. This has been aided by the introduction of the Paris–Edinburgh high-pressure cell[40]. Now, it is possible to carry out neutron diffraction studies up to 25 GPa (ref. 41).

It is well-known that high pressure reduces the atomic volume and in general brings the atoms closer to each other. This will happen for the hydrogen bonds as well. It is then possible that under pressure, other electro-negative atoms come near the vicinity of the hydrogen atom in the hydrogen bond and thus form bifurcated or multi-centred hydrogen bonds. Recent high pressure neutron diffraction studies have revealed these in water-containing minerals[47]; in the high pressure phase IV of ammonia[43] and in high pressure V-NaOD phase[44].

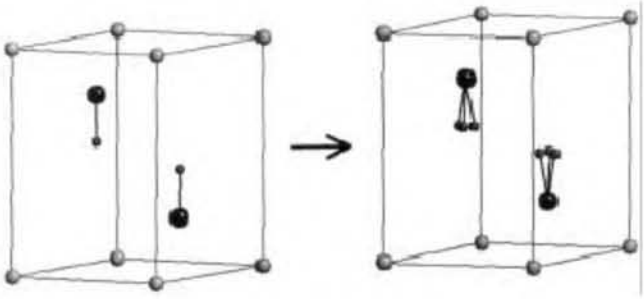

Figure 4. Transition from a single site to a three-site split-hydrogen model in $M(OH)_2$ compounds due to steric constraint arising from application of pressure.

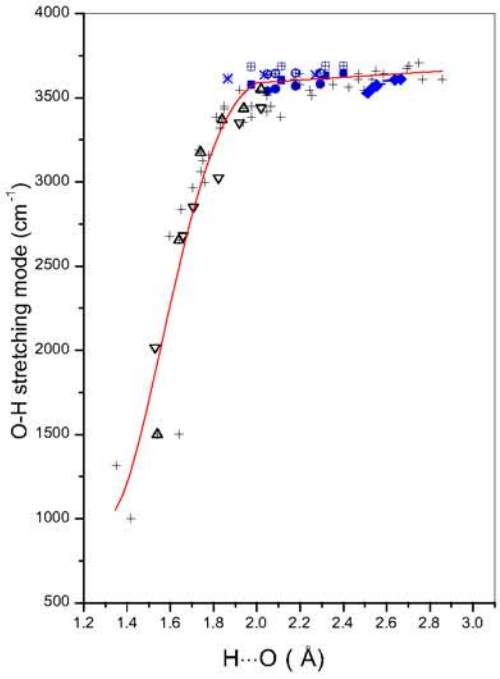

Figure 5. Frequencies of the O–H stretching mode versus H···O distance. Blue colour symbols represent high pressure data of $M(OH)_2$ oxides. Red curve is fit to the eye to 0.1 MPa data assembled by Jacobsen *et al.*[54] on different minerals.

Reduction of distances between atoms at high pressures can also lead to steric constraints[45]. For example, the decrease of distance X···Y may make the bonds more linear because of increased repulsive dispersive energy contribution. In cooperative hydrogen bond of type –X–H_1···Y–H_2···Z–, the neighbouring hydrogen atoms (say H_2) may approach the hydrogen atom, H_1 in the hydrogen bond under pressure and come closer than the sum of the van der Waals radii. This will then contribute an additional repulsive energy to the energy of the isolated hydrogen bond. At 2.05 Å, the limiting value[46] of the non-bonded H···H distance at 0.1 MPa, the repulsive energy is ~ 4 kJ/mol. Analysis of the available high pressure data shows that 0.1 MPa limiting-distance values nearly hold at high pressure also[47]. On attainment of the limiting distances at a pressure by the substance, phase transitions are detected. The crystal then lowers its free energy by going over to a new crystalline phase in which the H···H contacts are less repulsive. For example, in $Ni(OH)_2$ and other $M(OH)_2$ compounds[48], this repulsive H···H interaction results in hydrogen disorder, with the hydrogen atom moving away from the three-fold axis and taking a split three-site position with 1/3 occupancy (Figure 4). If no crystalline phase exists in the nearby free-energy landscape, the crystal vitrifies taking advantage of the higher configurational entropy in the amorphous phase[49]. In hydrates, there is possibility of a change in the lone-pair coordination of water molecules when another non-bonded atom comes into the proximity of the donor oxygen atom.

Another effect expected is the symmetrization of a hydrogen bond[50]. This follows from the 0.1 MPa correlation between X–H and X–H···X distances, assembled with data from different chemical substances. It involves the evolution of the lower-barrier, double-welled, hydrogen-bond potential into a single-well potential. Thus, pressure-tuning of hydrogen-bonded materials is a natural way of testing their potential functions. Recent studies on ice have addressed this question[51]. It is found that the 0.1 MPa X–H and X···Y correlation is not followed. In ice, the rate of increase of O–H is much smaller ($0.04 \pm$ pm GPa^{-1}) compared to the expected value (0.2 to 0.3 pm GPa^{-1}). Similar observations have been made for V–NaOD[44] and for N–H bond in ammonia IV (ref. 43). This also implies that the hydrogen-bond centring in ice should be observed at much higher pressures than predicted by the 0.1 MPa correlation. This is indeed found to be so by recent X-ray diffraction experiments done up to 170 GPa in conjugation with first principles molecular-dynamics simulations[52]. On the other hand, the 0.1 MPa correlation between O–H stretching frequency and H···O distance seems to hold at high pressures, as is shown in Figure 5. However, in some minerals, blue shift of the stretching frequency with pressure has been reported[53]. Proper interpretation of this

needs further precision investigations of their structures by neutron diffraction.

1. Gutberlet, T., Heinemann, U. and Steiner, M., *Acta Crystallogr., Sect. D*, 2001, **57**, 329–334.
2. Ramaseshan, S., *Curr. Sci.*, 1966, **35**, 87–91.
3. Ellison, R. D. and Levy, H. A., ORNL-4164, 1965, p. 126.
4. Sikka, S. K. and Chidambaram, R., *Acta Crystallogr., Sect. B*, 1969, **25**, 310–313.
5. Karle, J., *Acta Crystallogr.*, 1966, **20**, 881–886.
6. Sikka, S. K., *Acta Crystallogr., Sect. A*, 1969, **25**, 539–543; 1970, **26**, 662–666.
7. Ramanadham, M., Sikka, S. K. and Chidambaram, R., *Pramana*, 1973, **1**, 247–259.
8. Verbist, J. J., Lehmann, M. S., Koetzle, T. F. and Hamilton, W. C., *Nature*, 1972, **235**, 328–329.
9. Bernal, I. and Watkins, S. F., *Science*, 1972, **178**, 1282–1283.
10. Hauptman, H. A. and Langs, D. A., *Acta Crystallogr., Sect. A*, 2003, **59**, 250–254.
11. Johnson, C. K., ORNL-4168, 1967, p. 115.
12. Rossmann, M. G., *Acta Crystallogr.*, 1961, **14**, 383–388.
13. Peterson, S. W. and Smith, H. G., *J. Phys. Soc. Jpn B*, 1962, **17**, 335.
14. Dale, D. and Willis, B. T. M., AERE, 1966, R-5195.
15. Sikka, S. K., *Acta Crystallogr., Sect. A*, 1973, **29**, 211–212.
16. Chidambaram, R., Sequeira, A. and Sikka, S. K., *J. Chem. Phys.*, 1964, **41**, 3616–3622.
17. Momin, S. N. *et al.*, *Pramana*, 1978, **10**, 289–302.
18. Chidambaram, R., *Acta Crystallogr.,* 1961, **14**, 467–468.
19. Peterson, S. W. and Levy, H. A., *Acta Crystallogr.,* 1951, **10**, 70–76.
20. Chidambaram, R., *J. Chem. Phys*. 1962, **36**, 2361.
21. Chidambaram, R. and Sikka, S. K., *Chem. Phys. Lett.*, 1968, **2**, 162–165.
22. Chidambaram, R., Balasubramanian and Ramachandran, G. N., *Biochim. Biophys. Acta*, 1970, **221**, 182–195.
23. Ramanadham, M. and Chidambaram, R., In *Advances in Crystallography* (ed. Srinivasan, R.), Oxford and IBH, New Delhi, 1978, pp. 81–103.
24. Koetzle, T. F. and Lehman, M. S., In *The Hydrogen Bond II. Structure and Spectroscopy* (eds Schuster, P., Zundel, G. and Sandorfy, C.), North-Holland, Amsterdam, 1976, p. 457.
25. Olovsson, I. and Jonsson, P. G., In *The Hydrogen Bond II. Structure and Spectroscopy* (eds Schuster, P., Zundel, G. and Sandorfy, C.), North-Holland, Amsterdam, 1976, p. 393.
26. Savage, H. F. J. and Finney, J. L., *Nature*, 1986, **322**, 717–720.
27. Steiner, T. and Saenger, W., *Acta Crystallogr., Sect. B*, 1994, **50**, 348–357.
28. Chidambaram, R. and Ramanadham, M., *Physica B*, 1991, **174**, 300–305.
29. Brown, I. D. and Wu, K. K., *Acta Crystallogr., Sect. B*, 1976, **32**, 1957–1959.
30. Ramanadham, M., Siekar, L. C. and Jensen, L. H., *Acta Crystallogr., Sect. B*, 1990, **46**, 63–69.
31. Mason, S. A., Gentley, G. A. and McInytyre, G. J., In *Neutrons in Biology* (ed. Schoenborn, B. P.), Plenum, New York, 1984, pp. 323–334.
32. Schoenborn, B. P., *Nature*, 1969, **224**, 143–146.
33. Fong, S., Ramakrishnan, V. and Schoenborn, B. P., *Proc. Natl. Acac. Sci. USA*, 2002, **97**, 3872–3877.
34. Ostermann, A. *et al.*, *Biophys. Chem.*, 2002, **95**, 183–193.
35. Wilkinson, C. and Lehmann, M. S., *Nucl. Instrum. Methods*, 1991, **310**, 411–415.
36. Tanaka, I., Kurihara, K., Chatake, T. and Niimura, N., *J. Appl. Crystallogr.*, 2002, **35**, 34–40.
37. Tanaka, I., Ozebi, T., Ohhara, T., Kurihara, K. and Niimura, N., ICANS–XVI, 2003.
38. Kossiakoff, A. A. and Spencer, C.-A., *Nature*, 1980, **288**, 414–416.
39. Niimura, N. *et al.*, *Nature Struct. Biol.*, 1997, **4**, 909–917.
40. Besson, M. *et al.*, *Physica B*, 1992, **180 and 181**, 907–910.
41. Loveday, J. S. *et al.*, *High Press. Res.*, 1996, **14**, 303–309.
42. Northrup, P. A., Leinenweber, K. and Parise, J. B., *Am. Mineral.*, 1994, **79**, 401–404.
43. Loveday, J. S. *et al.*, *Phys. Rev. Lett.*, 1996, **76**, 74–78.
44. Loveday, J. S. *et al.*, *J. Phys*. (CM), 1996, **8**, L597–L604.
45. Sikka, S. K. and Sharma, S. M., *Curr. Sci.*, 1992, **63**, 317–320.
46. Steiner, T. and Saenger, W., *Acta Crystallogr., Sect. B*, 1992, **48**, 551–552.
47. Sikka, S. K., *Indian J. Pure Appl. Phys.*, 1997, **35**, 677–681.
48. Chitra, M., Sharma, S. M., Kulshreshtha, S. K. and Sikka, S. K., *Physica B*, 2001, **307**, 111–116.
49. Sharma, S. M. and Sikka, S. K., *Prog. Mater. Sci.*, 1996, **40**, 1–77.
50. Holzapfel, W. B., *J. Chem. Phys.*, 1972, **56**, 712–715.
51. Besson, J. M. *et al.*, *Phys. Rev. B*, 1994, **49**, 12540–12550.
52. Benoit, M., Romero, A. H. and Marx, D., *Phys. Rev. Lett.*, 2002, **89**, 1455011–1455014.
53. Lager, G. A., Ulmer, P., Miletich, R. and Marshall, W. G., *Am. Miner.*, 2001, **86**, 176–180.
54. Jacobsen, S. D., Smyth, J. R., Swope, R. J. and Sheldon, R. L., *Am. Miner.*, 2000, **85**, 745–752.
55. MacDonald, A. C. and Sikka, S. K., *Acta Crystallogr., Sect. B*, 1969, **25**, 1804–1811.
56. Sikka., S. K., *Acta Crystallogr., Sect. A*, 1969, **25**, 621–626.
57. Koetzle, T. F. and Hamiltton, W. C., In *Anomalous Scattering* (eds Ramaseshan, S. and Abrahams, S. C.), Munksgaard, Copenhagen, 1975, pp. 489–502.
58. Sikka, S. K. and Rajagopal, H., see ref. 57, pp. 503–519.
59. Bartunik, H. D. and Fuess, H., In Proceedings of Neutron Conference, Petten, 1975, p. 527.
60. Flook, R. J., Freeman, H. C. and Schudder, M. L., *Acta Crystallogr., Sect. B*, 1977, **33**, 801–809.
61. Scheoenborn, B. P., see ref. 57, pp. 407–415.

Received 19 September 2003